Soft Matter

Dynamic Article Links

Cite this: *Soft Matter*, 2012, **8**, 3982

www.rsc.org/softmatter

PAPER

Formation and dissolution of phospholipid domains with varying textures in hybrid lipo-polymersomes†

Jin Nam,[ab] T. Kyle Vanderlick[a] and Paul A. Beales*[c]

Received 20th March 2012, Accepted 19th June 2012
DOI: 10.1039/c2sm25646k

The design of novel, soft membrane structures with chemical and physical properties that are tunable across a broad spectrum of parameter space is important for the development of new functional materials. Many potential applications of these novel membranes will likely require biocompatible interfaces, *e.g.*, for functional reconstitution of integral proteins. Here we investigate the formation and control of compositional heterogeneities in hybrid lipo-polymersomes (HLPs) created by mixing the diblock copolymer poly(butadiene-*b*-ethylene oxide) with common natural lipids, *e.g.*, 1,2-dipalmitoyl-*sn*-glycero-3-phosphocholine or 1,2-palmitoyl-oleoyl-*sn*-glycero-3-phosphocholine. Mixing and de-mixing of lipid-rich domains from the polymer-rich matrix of hybrid vesicles is controlled *via* thermally driven phase separation and by the inclusion of cholesterol. Domain size and morphology can be controlled by cooling rate and lipid composition, respectively. Macromolecular additives, *e.g.*, cyclodextrins, enzymes and surfactants, can be used to remodel the hybrid membrane and its domains, resulting in domain dissolution, controlled release of contents or rupture of the hybrid vesicles. These composite membranes are promising materials for encapsulation-based technologies that require the combination of biocompatible membrane environments and enhanced structural stability, *e.g.*, delivery and sensing applications or controlling (bio)chemical reactions within confinement.

Introduction

As model cellular membranes, self-assembling block copolymers, known as polymersomes, are desirably tough (*i.e.*, with notable mechanical stability) but are generally lacking in inherent biocompatibility. While biodegradable copolymers have been developed for biomedical applications,[1–4] the biofunctionality of these synthetic membranes pales in comparison to phospholipid-based liposomes which share the same basic constituents as their cellular counterparts. Liposomes, for example, are readily used for the functional reconstitution of integral membrane proteins,[5,6] and multicomponent formulations can exhibit heterogeneities that mimic those found in biological systems.[7,8] Unfortunately, the lack of long-term stability of liposomes can be problematic for applications which require extended shelf-lives or prolonged monitoring times. In addition, membrane-specific interactions with various molecules in the host media can acutely perturb the structural integrity of liposomes.[9,10]

Given the interest in model membranes for various biotechnology applications as well as for fundamental studies, there is ample motivation to develop hybrid systems which bring together the excellent mechanical stability and chemical tunability of polymersomes with the inherent biocompatibility and biofunctionality of liposomes. Few studies to date have explored phospholipid/copolymer mixed vesicles despite the clear advantages of combining their best features.[11–15] For example, it has already been shown that such hybrid vesicles can enhance targeting efficiency in drug delivery applications.[16]

Our focus is on combining phospholipids and diblock copolymers to create novel hybrid lipo-polymersomes (HLPs) at the micron-scale in the form of giant unilamellar vesicles (GUVs), where basic morphological features can be revealed by optical microscopy. Recently we showed how receptor–ligand (avidin–biotin) interactions could be used to promote domain formation in HLPs,[17] creating, for example, lipid-rich domains encased within a polymer matrix. However, the biofunctionality of such domains may be limited by the protein coatings needed to form them.

In this paper, we demonstrate the formation of well-mixed HLPs that can be induced to demix to form lipid-rich domains without having to burden the system with receptor–ligand pairs that could limit membrane accessibility and the ultimate utility of these hybrid model membranes. Our objective was to identify simple

[a]*Chemical & Environmental Engineering, Yale University, New Haven, CT 06511, USA*
[b]*Amorepacific Corp. R&D Center. Giheung-gu, Yongin-si, Gyeonggi-do, Korea*
[c]*Centre for Molecular Nanoscience, School of Chemistry, University of Leeds, Leeds, LS2 9JT, UK. E-mail: p.a.beales@leeds.ac.uk; Tel: +44-(0)113-343-9101*

† Electronic supplementary information (ESI) available: Supporting confocal/epi-fluorescence microscopy images of HLP-GUVs. See DOI: 10.1039/c2sm25646k

polymer–lipid systems inclined to demix by phase separation and to understand how one can manipulate the resultant textures that form. Success is readily found by using different phospholipids (1,2-dipalmitoyl-*sn*-glycero-3-phosphocholine (DPPC) and 1,2-palmitoyl-oleoyl-*sn*-glycero-3-phosphocholine (POPC)), with the addition of cholesterol. We investigate how membrane composition and cooling rate can control the shape and size of these "biological windows" within the HLPs. Furthermore, we investigate sculpting these membranes by different external macromolecular stimuli and show potential applications of these hybrid vesicles in stimuli-triggered controlled release.

Experimental

Materials

1,2-di-lauryoyl-*sn*-glycero-3-phosphocholine (DLPC, $T_m \approx -1\,^{\circ}C$), 1,2-ditridecanoyl-*sn*-glycero-3-phosphocholine ($DC_{13}PC$, $T_m \approx 14\,^{\circ}C$), 1,2-di-palmitoy-*sn*-glycero-3-phosphocholine (DPPC, $T_m \approx 41\,^{\circ}C$), 1-palmitoyl-2-oleoyl-*sn*-glycero-3-phosphocholine (POPC, $T_m \approx -2\,^{\circ}C$), 1,2-dioleoyl-*sn*-glycero-3-phosphoethanolamine-*N*-(lissamine rhodamine B sulfonyl) (ammonium salt) (Rh-DOPE) and cholesterol (Chol) were purchased from Avanti Polar Lipids, Inc. (Alabaster, AL) and Oregon Green® 488 1,2-dihexadecanoyl-*sn*-glycero-3-phosphoethanolamine (OG-DHPE) was purchased from Invitrogen-Molecular Probes. Poly-(butadiene-*b*-ethylene oxide) (PBdPEO) diblock-copolymer was purchased from Polymer Source Inc. as a custom-synthesized material. Its overall molecular weight (M_w) was reported to be $\sim$3800 g mol^{-1} with 46 Bd units and 30 EO units. The poly-dispersity (PDI) was reported to be 1.04. (2-Hydroxypropyl)-β-cyclodextrins (β-CDs), Phospholipase A_2 (PLA_2) and other chemicals were purchased from Sigma of the highest grade available, and used as received.

HLP-GUVs preparation

Giant unilamellar vesicles (GUVs) were formed using a modification of the electroformation method.[18] Phospholipid (and, if relevant, cholesterol) was combined with PBdPEO and the chosen fluorescent lipids ($\sim$0.5 mol%) in chloroform (0.5 mg ml^{-1} total amphiphile concentration) at the desired molar ratios. 50 μl of lipid–copolymer mixed solution was spread on platinum electrodes that were held 8 mm apart in a home-built Teflon cell. Electroformation was carried out in a 260 mOsm sucrose solution. An alternating electric field was applied across the wires at 3 V A.C. and 15 Hz with a sine wave function.

Confocal microscopy

Vesicle observation was conducted in phosphate-buffered (pH 7.4) glucose solutions (265 mOsm). The external solution enhanced the optical contrast of vesicles due to the difference in refractive index with the encapsulated sucrose solution. The difference in densities between the vesicles' internal and external aqueous environments also caused the HLPs to sediment to the bottom of the sample dish, which aids the observation of these hybrid GUVs.

All images were acquired on a Leica TCS SP5 confocal microscope, equipped with LCS software and a Leica 40x/1.25-0.75 Plan Apo oil immersion objective lens. Rh-DOPE was excited by the 561 nm line of a DPSS laser and OG-DHPE and carboxyfluorescein were excited by the 488 nm line of an Ar laser. Samples were prepared in glass-bottom culture dishes (P35G-1.5-14-C; MatTek) coated with 5 wt% (/vol) bovine serum albumin solution for 1 h at room temperature prior to use, in order to prevent vesicles from adhering to the glass cover-slip. The temperature of microscope stage was controlled with warmed platforms (WP-10, WP-16; Harvard Apparatus).

For cholesterol-depletion studies using β-CD, HLPs (POPC:PBdPEO:Chol) were incubated with β-CD in a Tris-buffered sodium chloride solution (125 mM; pH 7.4) for 6 h at room temperature. Cholesterol depleted HLPs were separated from the β-CD solution by centrifugation prior to observation.

Confocal microscopy controlled release assay

HLP-GUVs were formed in 250 mM sucrose solution with 5,6-carboxyfluorescein (1 mg ml^{-1}). The lipopolymersome suspension (100 μl) was dispersed in glucose–HEPES buffer (1 ml of 250 mM, pH 7.2) containing 1 mM $CaCl_2$. The mixture was incubated for 2 h with 20 μl of highly purified phospholipase A_2 (from honey bee venom, 1 mg ml^{-1}) and was then observed under the confocal microscope.

Fluorescence spectroscopy controlled release assay

HLP-GUVs were formed with 250 mM sucrose solution with proteinase K (from *Tritirachium album*, 1 mg ml^{-1}). 100 μl of this lipo-polymersome suspension was dispersed in 1 ml of 0.25 M glucose–HEPES buffer (pH 7.2) containing 1 mM $CaCl_2$ and Bodipy–BSA (albumin from bovine serum, BODIPY® FL conjugate, 20 μg ml^{-1}). The mixture was incubated for 2 h with 20 μl of highly purified PLA_2 (1 mg ml^{-1}). Fluorescence spectra of the samples were measured using a fluorescence spectrophotometer with an excitation of 501 nm.

Results and discussion

In this section we describe the formation of lipid-rich domains in these hybrid membranes with attention to the effect of lipid constituent(s), composition, and sample cooling rates on the size, morphology and apparent phase of the resultant domains. We then investigate how these textured hybrid membranes respond to some common macromolecular stimuli that are well known to strongly interact with phospholipid model membranes. Our basic paradigm for engineering these hybrid systems is to incorporate lipids that, on their own, preferentially form highly ordered bilayer phases at ambient temperatures.

Formation of DPPC-rich domains *via* phase separation

The first lipid component we investigate is DPPC due to its thermally accessible phase transition at 41 °C.[19] Above this melting temperature, T_m, DPPC bilayers are fluid. Below it, the lipid tails undergo an ordering transition and the membranes convert to a condensed, more ordered state. When DPPC is incorporated into liposomes with other lipids that prefer to be in a fluid state at ambient conditions (*e.g.*, POPC, DOPC), these systems demix below the mixture's miscibility temperature with

DPPC-rich domains forming in the membrane.[20] Similarly, we show here that DPPC-rich domains also form in hybrid membranes with block copolymers.

HLPs are formed from mixtures of the diblock copolymer poly(butadiene-*b*-ethylene oxide) (PBdPEO) and DPPC. Single component GUVs can be readily formed with both species. These amphiphiles were mixed in chloroform and dried onto Pt wires under vacuum. HLP-GUVs were formed by electro-swelling at approximately 50 °C, above T_m of DPPC. The micron size of GUVs allows us to observe the miscibility and morphology of hybrid vesicles by confocal microscopy. Above the miscibility temperature of the hybrid system, homogenously mixed membranes are observed without visible domain formation (Fig. 1a). Uniform fluorescence intensity from the HLP-GUV membranes confirms that both amphiphilic molecules are miscible in the fluid state, without observable heterogeneities on length scales above the optical resolution of the microscope ($\approx$200 to 300 nm).

Upon cooling, which increases the lateral interactions between the lipids, we observe the formation of phospholipid-rich domains *via* phase separation (Fig. 1b) leading to micron-scale, star-like domains. The fluorescent lipid probe, Rh-DOPE, is largely excluded from the more ordered lipid-rich domains and concentrates in the fluid copolymer-rich matrix of the continuous phase. The ordered lipid domains are more rigid than the matrix and can even 'bulge' out from the smoothly curved polymer shell, locally deforming the shape of the copolymer matrix membrane; the arrow in the ESI Fig. S1† highlights this subtle effect. The rigid, solid-like lipid domains want to form flattened facets on the spherical vesicle, leading, in some instances, to observable deformation of the fluid block copolymer matrix.

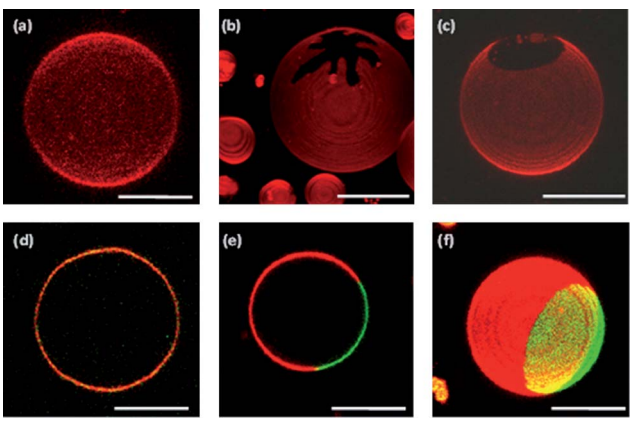

Fig. 1 Confocal microscopy images of HLPs: (a) homogeneously mixed HLP-GUVs composed of PBdPEO:DPPC (6 : 4) at ~50 °C; (b) irregular, star-shaped DPPC-rich domains in PBdPEO:DPPC (6 : 4) HLP-GUVs cooled to room temperature; (c) spherical shaped DPPC-rich domains in HLP-GUVs composed of PBdPEO:DPPC:Chol (5 : 3 : 2) cooled to room temperature; (d) HLP-GUV composed of PBdPEO:POPC (5 : 3) at room temperature with homogeneous surface texture; (e and f) PBdPEO: POPC:Chol (1 : 1 : 1) at room temperature. (a–c) show the red channel (Rh-DOPE, which preferentially partitions into the copolymer matrix); (d–f) are all superpositions of the red channel (Rh-DOPE) and the green channel (OG-DHPE, which partitions into POPC-rich domains). 3D reconstructed spherical projections of GUV image stacks are shown in (a–c and f); (d and e) are 2D confocal slices through the equator of the GUV. The scale bar represents 10 μm.

This thermally induced domain formation is reversible. When the temperature is increased above the miscibility temperature of the mixed membrane, the lipid rich domains dissolve, resulting in a homogeneous, single phase membrane.

Strategic variations in membrane composition allow us to manipulate the morphology of the resultant domains. In contrast to the irregular shapes described above, the incorporation of cholesterol in the hybrid membrane leads to the formation of domains with quasi-circular shapes, as shown in Fig. 1c for HLPs composed of PBdPEO:DPPC:Chol (5 : 3 : 2). We attribute this shape change to the known influence of cholesterol on lipid packing and associated lipid phase transitions. When introduced into solid-like lipid bilayers, cholesterol disrupts the lateral packing of the lipids causing positional/translational disordering of the lipids while still maintaining a high degree of orientational order.[21–23] At sufficient cholesterol compositions, solid-like lipid bilayers ultimately transform to a liquid-ordered (L_o) phase.[24–26] The rounded morphology of domains formed in these cholesterol-containing HLPs is likely a consequence of higher lipid mobility such that the domains can feasibly rearrange to minimize the line tension between coexisting phases.[27] A corroborating effect is the lack of any noticeable membrane deformations/bulging that are otherwise present when the more rigid cholesterol-free solid-like domains are embedded in the polymer-rich matrix (ESI, Fig. S1†). Despite their increased fluidity, these cholesterol-containing domains were not observed to coalesce on observational timescales, unlike the behaviour of liquid ordered domains in ternary lipid mixtures.[28] This is most likely, in part, to be due to the lower fluidity of block copolymer membranes, in comparison to liquid disordered lipid bilayers, which reduces the mobility of the domains in the continuous phase.[29]

Lipid domains rich in low T_m phospholipids

Whilst lipid-rich domains composed of high T_m lipids, like DPPC, might be useful for some applications, we also sought to create lipid "windows" rich in low T_m lipids, which are preferentially in a fluid state at room temperature. Low T_m phospholipids have short or unsaturated hydrophobic tails and form fluid (L_α) bilayers as unitary systems at ambient temperature, a state considered to be a similar environment to the majority structure of natural cell membranes.[30] We previously found that the lipid POPC ($T_m \approx -2$ °C), which is a major constituent of physiological cell membranes, forms well-mixed homogeneous membranes when mixed with PBdPEO (Fig. 1d). To induce demixing in this system, a protein-driven cross-linking process was required, which limits the biofunctionality of the resultant domains.[17]

Notably cholesterol is thought to complex with lipids in fluid L_α phases such that it increases orientational chain order and induces condensation of fluid phase lipids, enhancing their lateral interactions.[21–23] We find that the incorporation of cholesterol (>15 mol%) to create ternary PBdPEO/POPC/Chol HLPs does in fact elicit the formation of micron-scale POPC-rich domains (Fig. 1e and f). Lipid domain size can reach tens of microns (Fig. 1e) with a circular domain morphology that is characteristic of liquid phase domains. Domain size can be controlled *via* composition, *e.g.*, compare 5 : 3 : 3 to 3 : 5 : 2

PBdPEO:POPC:Chol HLPs (ESI, Fig. S2a and c†). We also find that cholesterol can induce domain formation within HLPs containing other low melting temperature lipids such as DLPC (ESI, Fig. S2d†) and $DC_{13}PC$.[31]

The exact phase of these low T_m lipid-rich domains is not certain. However, three reasons lead us to suggest that these domains are in a L_o-like state as opposed to a liquid-disordered, L_α, configuration. Firstly, the relatively high proportion of cholesterol required for domains to form in POPC-containing HLPs is consistent with reports of the formation of an L_o phase in binary POPC/cholesterol membranes.[32] Secondly, we were unable to create lipid-rich domains in HLPs containing DOPC ($T_m \approx -20$ °C) as the lipid component, even at very high cholesterol compositions: DOPC–Chol mixtures are not known to form L_o bilayers across their compositional space.[33,34] Finally, we find no significant differences between the domain partitioning preferences of lipophilic dyes in HLPs containing fluid-like DPPC/Chol domains and POPC/Chol domains: Rhodamine labeled DHPE and DOPE always preferentially partitioned into copolymer-rich phases, whilst perylene and NBD-DPPE preferred the lipid rich phases. These dye partitionings are consistent with their behaviours in ternary lipid mixtures, where the rhodamine dyes prefer the L_α phase while NBD and perylene prefer L_o domains.

Influence of cooling rate on domain size and morphology

Cooling kinetics control domain size; faster cooling rates result in the formation of smaller domains. This is demonstrated using PBdPEO/DPPC HLPs as shown in Fig. 2. While large micron-scale lipid domains are formed at 0.1 °C s^{-1}, a greater number of smaller micron-sized domains are formed at the faster cooling rate of 0.2 °C s^{-1}. At 0.4 °C s^{-1} many sub-micron sized lipid domains form, distributed throughout the hybrid membrane (Fig. 2c). Whilst cooling rate modulates sizes, the shapes of these domains retain their irregular morphology. Similar to the binary membranes in Fig. 2, the domain size in PBdPEO/DPPC/Chol HLPs could also be controlled by cooling rate: fast cooling results in smaller domains, while their quasi-circular domain shape is conserved (ESI, Fig. S3†).

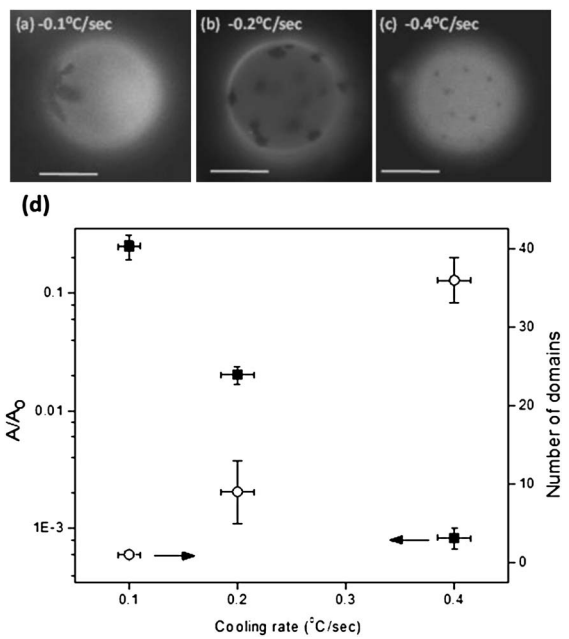

Fig. 2 Impact of cooling kinetics. (a–c) Epifluorescence microscopy images of HLPs (PBdPEO:DPPC (6 : 4) labelled with Rh-DOPE) prepared at different cooling rates. The scale bars represent 10 μm. (d) Number and apparent area fraction of individual domains (A/A_0) against cooling rate; A is the apparent area of individual domains and A_0 is the total area of observable membrane.

Classical nucleation theory readily describes the cooling rate effect: faster cooling rates result in a deeper thermal quench into the two phase coexistence region. This reduces the free energy barrier for nucleation and hence more domains form.[35–37] Assuming the surface fraction of lipid-rich domains approaches near equilibrium composition, the same area of lipid-rich phase distributed between a larger number of domains leads to a reduction in the average domain size within the HLPs. This effect is shown quantitatively in Fig. 2d. Apparent domain sizes have a relatively narrow distribution at each cooling rate, which is likely indicative of an instaneous nucleation mechanism, where all observed domains nucleate in an initial burst before domain growth dominates the subsequent phase separation.[35]

The domains that form upon cooling are stable: they are not observed to aggregate or ripen into larger domains during experimental timescales (a few days). This is likely a result of low mobility of domains in the continuous phase.[17] Therefore domain coalescence is unlikely to be a dominant mechanism for domain growth (although domains may grow into one another as seen in Fig. 2b), maintaining a relatively narrow domain size distribution during phase separation. However, if we now consider the total apparent area fractions of domains at each cooling rate, we find this to be 0.25 ± 0.06 at 0.1 °C s^{-1}, 0.18 ± 0.11 at 0.2 °C s^{-1}, but only 0.03 ± 0.01 at 0.4 °C s^{-1}. This apparent reduction in total domain area at our fastest cooling rate may indicate the presence of unobservable, sub-microscopic domains below the resolution of the optical microscope (~200 to 300 nm). Therefore the apparent size distribution of domains at 0.4 °C s^{-1} may not be as narrow as Fig. 2d suggests. This may also indicate a change in nucleation mechanism, where a broader size distribution of a large number of domains would likely be a result of a continuous nucleation mechanism where nucleation dominates over domain growth in the phase separation of the system.[35] This is still consistent with classical nucleation theory, where a deeper (faster) thermal quench decreases the free energy barrier for the formation of a critical nucleus until such point where nucleation can continually occur during phase separation.

Response of textured HLPs to membrane-active stimuli

Finally, we also investigate how the phase-separated hybrid membranes described herein can be strategically modified upon exposure to various molecular stimulants. Such remodelling of these systems may prove useful in developing environment-sensitive "triggered release" capsules. We first investigate the triggered dissolution of cholesterol-containing domains upon exposure to 2-hydroxypropyl-β-cyclodextrin (β-CD). β-CD is known to deplete cholesterol from cell membranes by extracting the cholesterol and hosting it within its relatively hydrophobic

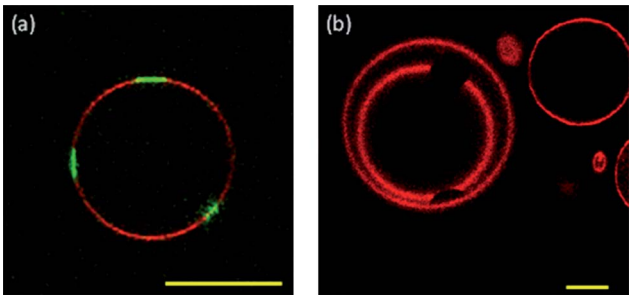

Fig. 3 Cholesterol-depletion of HLPs: (a and b) PBdPEO:POPC:Chol (4 : 3 : 3) at room temperature. (a) Lipid-rich domains are clearly visible before β-CD addition. (b) After β-CD addition lipid-rich domains are seen to have dissolved, however the lipid domains in the inner GUV did not disappear because β-CDs cannot approach the inner vesicle. The scale bars represent 10 μm.

inner cavity.[38,39] Using PBdPEO/POPC/Chol HLPs, we find that lipid-rich domains disappear after several hours of incubation with β-CD (Fig. 3): the reduced cholesterol composition within the membrane causes the phospholipids to redisperse into the polymer matrix, ultimately resulting in a homogeneous single phase HLP. Fig. 3b is particularly interesting as it shows one HLP nested within another: exposure to β-CD in the bathing solution causes the disappearance of the lipid domains from the outer HLP; however, as the β-CD cannot cross the membrane, domains persist within the inner HLP. As an aside, we note that the cholesterol–β-CD complexes form micelles in solution which can self-organize into helical ribbon structures (ESI Fig. S4†); similar β-CD superstructures have previously been reported, *e.g.*, during cholesterol monohydrate crystallization at low surfactant concentration.[40,41]

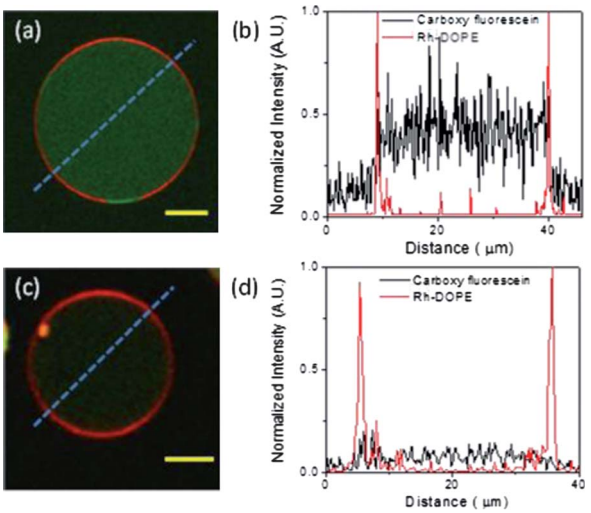

Fig. 4 Confocal images of carboxyfluorescein dye release from HLPs PBdPEO:DPPC:Cholesterol (5 : 3 : 2) (a) before and (c) after PLA_2 treatment (0.05 mg ml^{-1}). (b) and (d) represent the fluorescence intensities of Rh-DOPE and carboxyfluorescein along the line profiles shown in (a) and (c) respectively (blue dashed lines). After PLA_2 addition, carboxyfluorescein dyes are released from the HLPs as the lipid domains simultaneously dissolved. Note that these images represent two different HLPs from within the same sample. The scale bars represent 10 μm.

A second example of membrane restructuring serves to highlight the biofunctionality of the lipid-rich domains. In particular we expose the HLPs to the lipid enzyme phospholipase A_2 (PLA_2), which acts only on phospholipids cleaving their fatty acids from the *sn*-2 carbon of the glycerol backbone.[42] When PLA_2 is added to a solution containing PBdPEO/DPPC/Chol HLPs, the PLA_2 hydrolyzes phospholipid-rich domains only, leaving the copolymer-rich matrix intact (Fig. 4). As DPPC is hydrolysed, the lipid-rich domains are digested and the surrounding block copolymer matrix closes up to reseal the HLP membrane.

As a mock "triggered-release" system, Fig. 4 shows release of carboxyfluorescein dyes ($M_w \approx 0.38$ kDa) from self-healing HLPs as its lipid domains are digested by PLA_2. A more sophisticated HLP release system is created by releasing encapsulated proteinase K ($M_w \approx 28.9$ kDa), which is an enzyme that digests proteins. These proteinase loaded HLPs are incubated in

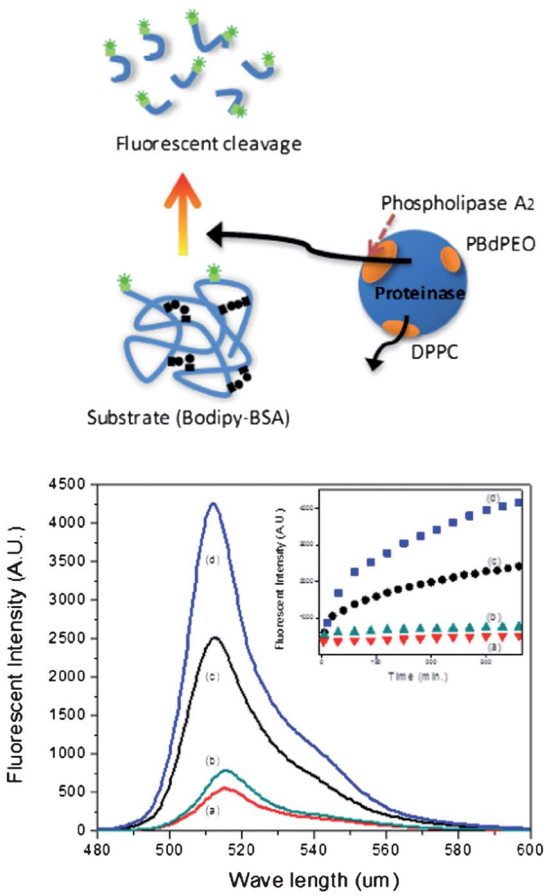

Fig. 5 [top] Schematic illustration of stimulus-triggered control release from HLPs. Proteinase K is released through phospholipid domains of HLPs, which are disintegrated by the trigger, PLA_2. The released enzyme is detected *via* the disruption of intra-molecular self-quenching of Bodipy–BSA. [bottom] The fluorescence intensity from the Bodipy moiety increases with increased release of proteinase K from the HLPs: (a) PBdPEO polymersomes with encapsulated proteinase K; (b) HLPs PBdPEO:DPPC:Cholesterol (5 : 4 : 3) with encapsulated proteinase K but without PLA_2 addition; (c) as (b) except with PLA_2 (0.05 mg ml^{-1}); (d) as (b) except with 3 times higher concentration of PLA_2 (0.15 mg ml^{-1}). The kinetics of the increase in Bodipy fluorescence intensity for each case are shown in the inset graph.

a buffer containing a fluorescent probe–protein conjugate: Bodipy–BSA. The attachment of the Bodipy fluorescent moiety to the BSA protein quenches its fluorescence.[43–45] Hydrolysis of the lipid domains by PLA_2 causes release of the encapsulated proteinase, which is detected as an increase in fluorescence intensity from the sample due to proteolysis of the Bodipy–BSA conjugate (Fig. 5). The action of PLA_2 on the HLPs (5 : 3 : 2 PBdPEO:DPPC:cholesterol) is found to be essential for proteinase action on the Bodipy–BSA. Expectedly, the PLA_2 enzyme is found to be completely ineffective when acting upon unitary polymersomes made from PBdPEO. The rate of release of proteinase from the HLPs is shown to be dependent upon the concentration of PLA_2: a three-fold increase in concentration of PLA_2 results in a significant increase in fluorescence signal (Fig. 5c and d). This assay confirms the controlled release of encapsulated biomolecules from HLPs upon digestion of the lipid domains by phospholipase enzymes.

The phase structure and size of lipid-rich domains influence the extent of contents release during PLA_2 hydrolysis. Domain phase structure is controlled *via* membrane composition: unsurprisingly L_o domains are more susceptible to PLA_2 hydrolysis than solid-like domains, leading to a greater extent of proteinase release and hence increased Bodipy fluorescence (Fig. 6a). Domain size is controlled *via* cooling rate: larger domains result in greater proteinase release from the HLPs

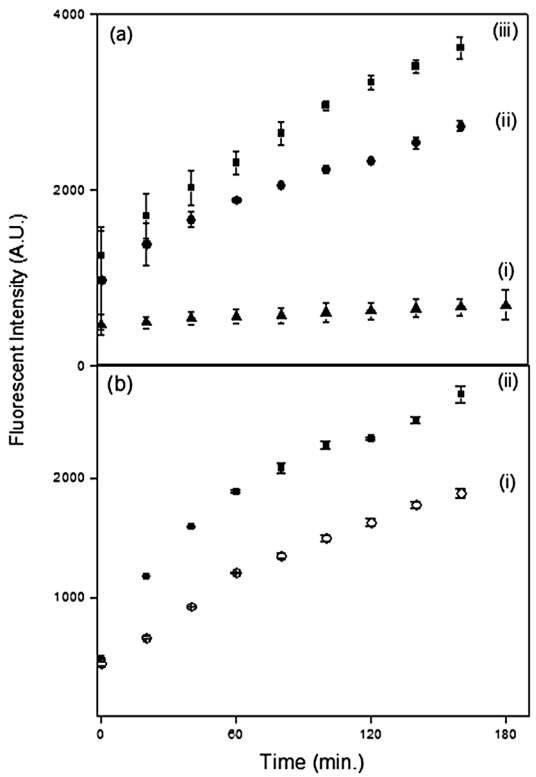

Fig. 6 Impact of domain phase and size on PLA_2 (0.05 mg ml^{-1}) triggered release at room temperature. (a) Domain phase as determined by membrane composition modulates the extent of protease release: (i) no domains (PBdPEO polymersomes), (ii) solid-like domains (3 : 2 PBdPEO:DPPC), (iii) L_o domains (5 : 4 : 3 PBdPEO:DPPC:cholesterol). (b) Domain size, determined by cooling rate, influences extent of protease release from 3 : 2 PBdPEO:DPPC HLPs: (i) 0.4 °C s^{-1}, (ii) 0.1 °C s^{-1}.

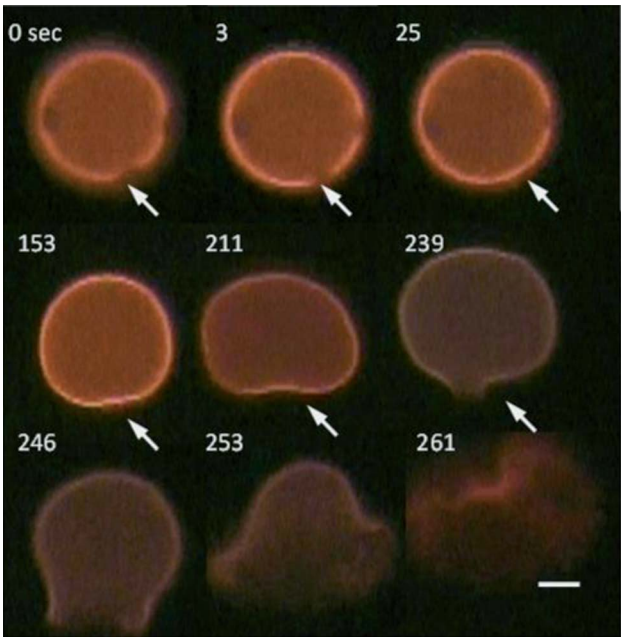

Fig. 7 HLP response to detergent action. Confocal microscopy images of a time series of PBdPEO:DPPC:Chol (5 : 3 : 2) HLPs treated with non-ionic surfactant (Triton X-100). Breaking and resealing of lipid domains are indicated by the white arrow. The scale bar represents 10 μm. Lipid-rich domains are more susceptible to the detergent. Non-fluorescent phospholipid-rich domains disintegrated first, forming pores which are simultaneously resealed by the surrounding polymer matrix. The HLP begins to deform from its spherical morphology (*e.g.* 211 s). Finally (239 s onwards), the HLP breaks open due to detergent action on the hybrid membrane.

(Fig. 6b), likely due to slower self-healing times from the block copolymer matrix for larger individual domains. As a corollary to the effect of lipid phase, we investigate the effect of PLA_2 activity when increasing the temperature to melt solid-like lipid domains at 45 °C (ESI, Fig. S5†). During the domain melting and dissolution there is significant increase in proteinase release from the HLPs; however there is also likely to be a contribution to the rapid increase in Bodipy fluorescence from increased enzymatic activity of the proteinase at higher temperatures.

Synthetic detergent (Triton X-100) can also be used to break up the lipid domains (Fig. 7). The molecular shape of detergents determines the manner in which they destabilize GUVs.[46–48] The bulky PEG headgroup of Triton X-100 causes these detergents to organize into micellar aggregates in aqueous solutions. In the presence of lipid bilayers, Triton X-100 forms mixed micelles with the lipids, solubilising the membrane. We find that Triton X-100 quickly disintegrates lipid-rich domains of PBdPEO/DPPC/Chol HLPs, forming holes that are quickly resealed by the surrounding polymer matrix. While the copolymer matrix is more resistant than the lipid-rich domains, at sufficiently high detergent concentrations (above 2% Triton X-100), the polymer vesicle peels open with the catastrophic loss of encapsulated volume. This process occurs on the time-scale of several minutes. Such an abrupt loss of contents (burst release) from HLPs may not be ideal for many controlled release applications where a slow release of contents over time would be more desirable.

Conclusions

In conclusion, we have demonstrated the design and application of novel, heterogeneous lipo-polymersome capsules. Phase-separation can be induced by temperature changes and/or introduction of cholesterol. Homogeneous HLPs form above the miscibility transition temperatures of the mixtures. Upon cooling, demixing of lipid and copolymer species is achieved. Lipid-rich domains with either solid-like or fluid-like characteristics nucleate and grow within the copolymer-rich continuous phase. The size and morphology of these domains can be controlled by cooling rate and membrane composition, respectively. These soft, self-assembled membrane structures combine the mechanical stability of polymersomes with the biofunctionality of lipid membranes within a micron-sized GUV architecture.[17] The lipid domains and polymer matrix of HLPs showed different stabilities against external stimuli (detergents and enzymes). The differences in membrane stability can be useful for various applications. The weaker but bio-compatible lipid membrane supports an optimum environment for the activity of biological molecules, while the sturdy polymer matrix provides structural stability to the system. This system exhibits two types of release mechanisms: bio-specific digestion of lipid domains by phospholipase activity results in slow release of contents accompanied by membrane self-healing through the block copolymer matrix, whilst harsh detergent action eventually breaks open (bursts) the HLPs leading to an abrupt release of contents. These HLPs could find applications as new, versatile delivery platforms by exploiting their various attributes: (1) ability to open/close the "biological windows" *via* various molecular triggers; (2) possibilities of incorporating integral membrane proteins into the biocompatible lipid domains; and (3) the potential to fine tune the physical and chemical properties of the polymer matrix through modification of the chemical and structural identity of the block copolymer constituents.

Notes and references

1 F. Ahmed and D. E. Discher, *J. Controlled Release*, 2004, **96**, 37–53.
2 H. Lomas, I. Canton, S. MacNeil, J. Du, S. P. Armes, A. J. Ryan, A. L. Lewis and G. Battaglia, *Adv. Mater.*, 2007, **19**, 4238–4243.
3 H. Lomas, M. Massignani, K. A. Abdullah, I. Canton, C. Lo Presti, S. MacNeil, J. Du, A. Blanazs, J. Madsen, S. P. Armes, A. L. Lewis and G. Battaglia, *Faraday Discuss.*, 2008, **139**, 143–159.
4 M. Massignani, C. LoPresti, A. Blanazs, J. Madsen, S. P. Armes, A. L. Lewis and G. Battaglia, *Small*, 2009, **5**, 2424–2432.
5 N. Kahya, E. I. Pecheur, W. P. de Boeij, D. A. Wiersma and D. Hoekstra, *Biophys. J.*, 2001, **81**, 1464–1474.
6 T. J. McIntosh and S. A. Simon, in *Annual Review of Biophysics and Biomolecular Structure*, 2006, vol. 35, pp. 177–198.
7 C. M. Paleos and D. Tsiourvas, *J. Mol. Recognit.*, 2006, **19**, 60–67.
8 M. Delcea, A. Yashchenok, K. Videnova, O. Kreft, H. Moehwald and A. G. Skirtach, *Macromol. Biosci.*, 2010, **10**, 465–474.
9 I. Bivas, M. Winterhalter, P. Meleard and P. Bothorel, *Europhys. Lett.*, 1998, **41**, 261–266.
10 C. Allen, N. Dos Santos, R. Gallagher, G. N. C. Chiu, Y. Shu, W. M. Li, S. A. Johnstone, A. S. Janoff, L. D. Mayer, M. S. Webb and M. B. Bally, *Biosci. Rep.*, 2002, **22**, 225–250.
11 T. Ruysschaert, A. F. P. Sonnen, T. Haefele, W. Meier, M. Winterhaltert and D. Fournier, *J. Am. Chem. Soc.*, 2005, **127**, 6242–6247.
12 Z. Cheng and A. Tsourkas, *Langmuir*, 2008, **24**, 8169–8173.
13 E. Amado and J. Kressler, *Curr. Opin. Colloid Interface Sci.*, 2011, **16**, 491–498.
14 S. Pispas, *Soft Matter*, 2011, **7**, 8697–8701.
15 M. Schulz, D. Glatte, A. Meister, P. Scholtysek, A. Kerth, A. Blume, K. Bacia and W. H. Binder, *Soft Matter*, 2011, **7**, 8100–8110.
16 Z. Cheng, D. R. Elias, N. P. Kamat, E. D. Johnston, A. Poloukhtine, V. Popik, D. A. Hammer and A. Tsourkas, *Bioconjugate Chem.*, 2011, **22**, 2021–2029.
17 J. Nam, P. A. Beales and T. K. Vanderlick, *Langmuir*, 2011, **27**, 1–6.
18 M. I. Angelova and D. S. Dimitrov, *Faraday Discuss.*, 1986, **81**, 303.
19 D. L. Melchior, F. J. Scavitto and J. M. Steim, *Biochemistry*, 1980, **19**, 4828–4834.
20 V. D. Gordon, P. A. Beales, Z. Zhao, C. Blake, F. C. MacKintosh, P. D. Olmsted, M. E. Cates, S. U. Egelhaaf and W. C. K. Poon, *J. Phys.: Condens. Matter*, 2006, **18**, L415–L420.
21 P. L.-G. Chong, W. Zhu and B. Venegas, *Biochim. Biophys. Acta, Biomembr.*, 2009, **1788**, 2–11.
22 D. Marsh, *Biochim. Biophys. Acta, Biomembr.*, 2009, **1788**, 2114–2123.
23 T. P. W. McMullen, R. Lewis and R. N. McElhaney, *Curr. Opin. Colloid Interface Sci.*, 2004, **8**, 459–468.
24 S. L. Veatch and S. L. Keller, *Biophys. J.*, 2003, **85**, 3074–3083.
25 J. R. Rubenstein, B. A. Smith and H. M. McConnell, *Proc. Natl. Acad. Sci. U. S. A.*, 1979, **76**, 15–18.
26 J. H. Ipsen, G. Karlstrom, O. G. Mouritsen, H. Wennerstrom and M. J. Zuckermann, *Biochim. Biophys. Acta*, 1987, **905**, 162–172.
27 C. Dietrich, L. A. Bagatolli, Z. N. Volovyk, N. L. Thompson, M. Levi, K. Jacobson and E. Gratton, *Biophys. J.*, 2001, **80**, 1417–1428.
28 S. L. Veatch and S. L. Keller, *Phys. Rev. Lett.*, 2002, **89**, 4.
29 J. C. M. Lee, M. Santore, F. S. Bates and D. E. Discher, *Macromolecules*, 2002, **35**, 323–326.
30 K. Simons and W. L. C. Vaz, *Annu. Rev. Biophys. Biomol. Struct.*, 2004, **33**, 269–295.
31 R. Lipowsky and E. Sackmann, *Structure and Dynamics of Membranes*, 1995, vol. 1A–1B.
32 R. F. M. de Almeida, A. Fedorov and M. Prieto, *Biophys. J.*, 2003, **85**, 2406–2416.
33 J. Zhao, J. Wu, F. A. Heberle, T. T. Mills, P. Klawitter, G. Huang, G. Costanza and G. W. Feigenson, *Biochim. Biophys. Acta, Biomembr.*, 2007, **1768**, 2764–2776.
34 S. L. Veatch and S. L. Keller, *Biochim. Biophys. Acta*, 2005, **1746**, 172–185.
35 D. Kashchiev, A. Borissova, R. B. Hammond and K. J. Roberts, *J. Phys. Chem. B*, 2010, **114**, 5441–5446.
36 D. Kashchiev, A. Borissova, R. B. Hammond and K. J. Roberts, *J. Cryst. Growth*, 2010, **312**, 698–704.
37 R. Lipowsky and R. Dimova, *J. Phys.: Condens. Matter*, 2003, **15**, S31–S45.
38 M. V. Rekharsky and Y. Inoue, *Chem. Rev.*, 1998, **98**, 1875–1917.
39 E. P. C. Kilsdonk, P. G. Yancey, G. W. Stoudt, F. W. Bangerter, W. J. Johnson, M. C. Phillips and G. H. Rothblat, *J. Biol. Chem.*, 1995, **270**, 17250–17256.
40 Y. V. Zastavker, N. Asherie, A. Lomakin, J. Pande, J. M. Donovan, J. M. Schnur and G. B. Benedek, *Proc. Natl. Acad. Sci. U. S. A.*, 1999, **96**, 7883–7887.
41 B. Khaykovich, C. Hossain, J. J. McManus, A. Lomakin, D. E. Moncton and G. B. Benedek, *Proc. Natl. Acad. Sci. U. S. A.*, 2007, **104**, 9656–9660.
42 O. G. Berg, M. H. Gelb, M. D. Tsai and M. K. Jain, *Chem. Rev.*, 2001, **101**, 2613–2653.
43 S. I. Simon, Y. Hu, D. Vestweber and C. W. Smith, *J. Immunol.*, 2000, **164**, 4348–4358.
44 J. A. Opdenkam, J. Degier and L. L. Vandeene, *Biochim. Biophys. Acta*, 1974, **345**, 253–256.
45 A. L. Kindzelskii, M. J. Zhou, R. P. Haugland, L. A. Boxer and H. R. Petty, *Biophys. J.*, 1998, **74**, 90–97.
46 F. M. Menger and M. I. Angelova, *Acc. Chem. Res.*, 1998, **31**, 789–797.
47 T. P. Sudbrack, N. L. Archilha, R. Itri and K. A. Riske, *J. Phys. Chem. B*, 2011, **115**, 269–277.
48 T. Toyota, H. Tsuha, K. Yamada, K. Takakura, K. Yasuda and T. Sugawara, *Langmuir*, 2006, **22**, 1976–1981.

